Cognitive Radar for Target Tracking Using a Software Defined Radar System

Kristine L. Bell*, Joel T. Johnson†, Graeme E. Smith†, Christopher J. Baker†, and Muralidhar Rangaswamy‡
*Metron, Inc., 1818 Library St., Suite 600, Reston, Virginia 20190, USA
†Dept. of Electrical and Computer Engineering and ElectroScience Laboratory, The Ohio State University, Columbus, Ohio, 43210, USA
‡U.S. Air Force Research Laboratory, Sensors Directorate, Radar Signal Processing Branch, Wright-Patterson AFB, OH, USA

***Abstract*—Most radar systems employ a feed-forward processing chain in which they first perform some low-level processing of received sensor data to obtain target detections and then pass the processed data on to some higher-level processor such as a tracker. Cognitive radar systems use adaptation between the information extracted from the sensor/processor and the design and transmission of subsequent illuminating waveforms. In this paper, we develop a cognitive radar tracking system based on the Maximum a Posteriori Penalty Function (MAP-PF) tracking methodology, which allows us to cognitively control both the radar sensor and the processor. We demonstrate performance for a pulse-Doppler radar system in which the pulse repetition frequency is adjusted to optimize tracking performance, while keeping the target from being Doppler-aliased and away from the zero-Doppler clutter. Results are shown on experimentally collected data using a software defined radar system.**

I. Introduction

Most radar systems employ a feed-forward processing chain in which they first perform some low-level processing of received sensor data to obtain target detections and then pass the processed data on to some higher-level processor (such as a tracker or classifier), which extracts information (such as target kinematic parameters and target type) to achieve a system objective. Tracking and classification can be improved using adaptation between the information extracted from the sensor/processor and the design and transmission of subsequent illuminating waveforms. As such, cognitive systems offer much promise for improved performance [1]-[4].

In [5] and [6], we developed a general cognitive sensor/processor system framework for a system engaged in target tracking. The model included the lower-level radar processor (detector) in the sensor and the higher-level task processor (tracker) in the processor. In [5], the framework was specialized for a task processor whose objective was single target state estimation (tracking), while in [6], it was specialized for target detection and track initiation/termination.

In this paper, we further develop the framework by assuming that the sensor supplies raw sensor data to the processor, which now includes both the detector and the tracker. We use the Maximum a Posteriori Penalty Function (MAP-PF) tracking methodology [7]-[8], which employs a two-step track estimation process similar to traditional feed-forward detection-based systems, except the processes are coupled via the penalty function and the data association step of traditional tracking approaches is eliminated. In the detection process, the penalty function uses the current target state estimate to guide the detector to the relevant region of the detection surface. In the track estimation process, the penalty function determines the influence of the detector measurements on the final track estimates by adaptively adjusting the measurement error variance. This formulation allows us to cognitively control both the sensor and processor for improved performance.

We demonstrate performance for a pulse-Doppler radar system in which the pulse repetition frequency (PRF) is adjusted to optimize tracking performance, while keeping the target from being Doppler-aliased and away from the zero-Doppler clutter. Results are shown on experimentally collected data using a software defined radar (SDR) system [9]-[10].

This work was supported by the U.S. Air Force Research Laboratory under contract FA8650-13-M-1656. Opinions, interpretations, conclusions, and recommendations are those of the authors and not necessarily endorsed by the U. S. Government.

II. Cognitive Sensor/Processor System Framework

A. System Model

The mathematical model of a cognitive sensor/processor system is shown in Figure 1. As in [5], the system consists of four components: the scene, which includes the target and the environment, the sensor that observes the scene, the processor that converts the observed data into a perception of the scene, and the controller that determines the next actions taken by the sensor and processor. In this paper, we assume that the sensor includes the transmitter and receiver and that the processor includes the detector and tracker.

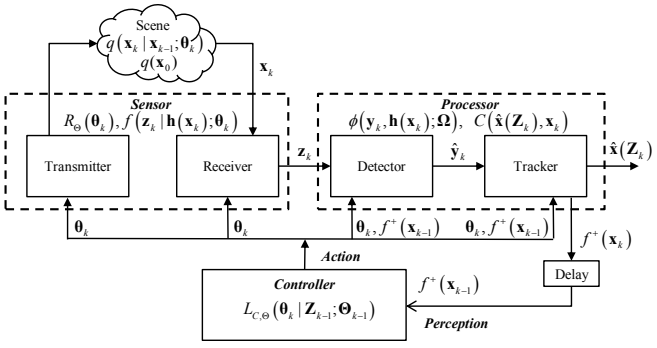

Fig. 1. **Cognitive Sensor/Processor System**

We assume that the objective of the system is to estimate the state of a target in the scene. The target state at time t_k is denoted as $\mathbf{x}_k$. The sensor observes the scene and produces a measurement vector $\mathbf{z}_k$ that depends on the target state $\mathbf{x}_k$ and the sensor parameters $\boldsymbol{\theta}_k$. We assume that the estimate of the target state at time t_k is a function of the observations up to time t_k, which in turn depend on the sensor parameters up to time t_k, which we denote as $\mathbf{Z}_k \equiv \{\mathbf{z}_1, \mathbf{z}_2, \ldots, \mathbf{z}_k\}$ and $\boldsymbol{\Theta}_k \equiv \{\boldsymbol{\theta}_1, \boldsymbol{\theta}_2, \ldots, \boldsymbol{\theta}_k\}$, respectively.

We assume a Markov motion model with initial target state probability density function (PDF) $q(\mathbf{x}_0)$ and the transition PDF $q(\mathbf{x}_k|\mathbf{x}_{k-1};\boldsymbol{\theta}_k)$. The transition density may depend on the sensor

parameters. This will occur, for example, when the choice of sensor parameters affects the time difference $\Delta t_k = t_k - t_{k-1}$.

The sensor measurement model is described by the likelihood function. The MAP-PF methodology applies to problems in which the likelihood function depends on the target state vector only through a known, possibly nonlinear mapping to the "natural parameters" of the sensor. In radar systems, the state parameters are typically the target position and velocity, while the natural parameters of the sensor are typically the angle, range, and/or Doppler frequency. Let $\mathbf{y}_k$ denote the natural parameters. They are related to the state parameters by the mapping

$$\mathbf{y}_k = \mathbf{h}(\mathbf{x}_k). \tag{1}$$

Let $f(\mathbf{z}_k|\mathbf{y}_k;\boldsymbol{\theta}_k)$ denote the likelihood function in terms of the natural parameters and $f(\mathbf{z}_k|\mathbf{h}(\mathbf{x}_k);\boldsymbol{\theta}_k)$ denote the likelihood function in terms of the state parameters. The cost of obtaining an observation and any constraints on the sensor parameters are modeled by the sensor cost function $R_\Theta(\boldsymbol{\theta}_k)$.

The processor processes the data and produces an estimate of the target state $\hat{\mathbf{x}}_k(\mathbf{Z}_k)$ by minimizing the expected value of the processor cost function $C(\hat{\mathbf{x}}_k(\mathbf{Z}_k), \mathbf{x}_k)$.

The controller decides on the next value for the sensor parameters $\boldsymbol{\theta}_k$ by minimizing a loss function $L_{C,\Theta}(\cdot)$ that balances the performance of the processor via the processor cost function $C(\cdot,\cdot)$ and the cost of using the sensor via the sensor cost function $R_\Theta(\cdot)$.

B. MAP-PF Tracking Processor

For tracking, we define the processor cost function to be the sum of the squared estimation errors [5], which is given by:

$$C\left(\hat{\mathbf{x}}(\mathbf{Z}_k), \mathbf{x}_k\right) = \text{tr}\left\{\left[\hat{\mathbf{x}}(\mathbf{Z}_k) - \mathbf{x}_k\right]\left[\hat{\mathbf{x}}(\mathbf{Z}_k) - \mathbf{x}_k\right]^T\right\}. \tag{2}$$

The optimal estimator, which minimizes the conditional Bayes risk, is the conditional mean [11]:

$$\hat{\mathbf{x}}(\mathbf{Z}_k) = \boldsymbol{\mu}_k^+ \equiv E_k^+\{\mathbf{x}_k\}, \tag{3}$$

where $E_k^+\{\cdot\}$ denotes expectation with respect to the posterior density $f^+(\mathbf{x}_k) \equiv f(\mathbf{x}_k|\mathbf{Z}_k;\boldsymbol{\Theta}_k)$.

For the Markov motion model, the posterior density may be obtained from the standard Bayes-Markov recursion [8], in which we first compute the predicted density $f^-(\mathbf{x}_k) \equiv f(\mathbf{x}_k|\mathbf{Z}_{k-1};\boldsymbol{\Theta}_k)$ using the Chapman-Kolmogorov equation, and then the posterior density using Bayes' rule. The recursion is initialized with

$$f^+(\mathbf{x}_0) = q(\mathbf{x}_0), \tag{4}$$

and then proceeds according to:

$$f^-(\mathbf{x}_k) = \int q(\mathbf{x}_k|\mathbf{x}_{k-1};\boldsymbol{\theta}_k) f^+(\mathbf{x}_{k-1}) d\mathbf{x}_{k-1} \tag{5}$$

$$f^+(\mathbf{x}_k) = \frac{f(\mathbf{z}_k|\mathbf{h}(\mathbf{x}_k);\boldsymbol{\theta}_k) f^-(\mathbf{x}_k)}{\int f(\mathbf{z}_k|\mathbf{h}(\mathbf{x}_k);\boldsymbol{\theta}_k) f^-(\mathbf{x}_k) d\mathbf{x}_k}. \tag{6}$$

The MAP-PF algorithm performs the same motion update as in (5), but breaks up the information update in (6) into three steps using the penalty function. The penalty function $\phi(\mathbf{y}, \mathbf{h}(\mathbf{x}))$ has the property that it is equal to zero when $\mathbf{y} = \mathbf{h}(\mathbf{x})$ and becomes smaller (more negative) as the distance between $\mathbf{y}$ and $\mathbf{h}(\mathbf{x})$ and increases. In this paper, we use the quadratic penalty function, defined as:

$$\phi(\mathbf{y}, \mathbf{h}(\mathbf{x}); \boldsymbol{\Omega}) = -\frac{1}{2}\left[\mathbf{y} - \mathbf{h}(\mathbf{x})\right]^T \boldsymbol{\Omega}^{-1}\left[\mathbf{y} - \mathbf{h}(\mathbf{x})\right], \tag{7}$$

where $\boldsymbol{\Omega}$ is a matrix chosen to weight the components of the penalty function in some desirable manner.

The three-step MAP-PF information update is given by [7]-[8]:

$$\hat{\mathbf{x}}_k^- = \arg\max_{\mathbf{x}_k} f^-(\mathbf{x}_k) \tag{8}$$

$$\hat{\mathbf{y}}_k = \arg\max_{\mathbf{y}} \ln f(\mathbf{z}_k|\mathbf{y};\boldsymbol{\theta}_k) + \phi\left(\mathbf{y}, \mathbf{h}(\hat{\mathbf{x}}_k^-); \boldsymbol{\Omega}\right) \tag{9}$$

$$f^+(\mathbf{x}_k) = \frac{\exp\left\{\phi\left(\hat{\mathbf{y}}_k, \mathbf{h}(\mathbf{x}_k); \boldsymbol{\Omega}\right)\right\} f^-(\mathbf{x}_k)}{\int \exp\left\{\phi\left(\hat{\mathbf{y}}_k, \mathbf{h}(\mathbf{x}_k); \boldsymbol{\Omega}\right)\right\} f^-(\mathbf{x}_k) d\mathbf{x}_k}. \tag{10}$$

In the first step, the MAP estimate of the predicted density is found. Depending on the implementation, it may be easier to find the minimum mean square error (MMSE) estimate, which is the mean of the predicted density, instead.

In the second step, the optimization problem in (9) is a penalized maximum likelihood (ML) problem. It can also be interpreted as a MAP estimation problem with the penalty function appearing where the prior term $\ln f(\mathbf{y})$ would appear. In a traditional feed-forward detection-based tracking system, the optimal detector would solve the standard ML problem (i.e. (9) without the penalty function) to get the detector measurement. In MAP-PF, the penalty function restricts the detector estimate to be in the vicinity of where the tracker predicts it to be, hence MAP-PF is performing guided detection. By specifying a quadratic penalty function, we are implicitly modeling the prior distribution of $\mathbf{y}_k$ as Gaussian with mean $\mathbf{h}(\hat{\mathbf{x}}_k^-)$ and covariance matrix $\boldsymbol{\Omega}$. We have some flexibility in choosing $\boldsymbol{\Omega}$, and a logical choice would be the predicted covariance matrix of $\mathbf{y}_k$, which we denote as $\boldsymbol{\Sigma}_{\mathbf{y}_k}^-$. This may be obtained from the predicted covariance of $\mathbf{x}_k$, denoted by $\boldsymbol{\Sigma}_k^-$, using a locally linear approximation of the function $\mathbf{h}(\mathbf{x})$ at the point $\hat{\mathbf{x}}_k^-$ as follows:

$$\boldsymbol{\Omega}_{\text{MAP},k} = \boldsymbol{\Sigma}_{\mathbf{y}_k}^- \cong \mathbf{H}(\hat{\mathbf{x}}_k^-)\boldsymbol{\Sigma}_k^-\mathbf{H}(\hat{\mathbf{x}}_k^-)^T, \tag{11}$$

where $\mathbf{H}(\hat{\mathbf{x}}_k^-)$ is the Jacobian matrix, defined as:

$$\mathbf{H}(\hat{\mathbf{x}}_k^-) = \left[\boldsymbol{\nabla}_{\mathbf{x}}\mathbf{h}(\mathbf{x})^T\right]\Big|_{\mathbf{x}=\hat{\mathbf{x}}_k^-}. \tag{12}$$

The third step in (10) looks like a standard information update with $\hat{\mathbf{y}}_k$ acting as the measurement vector and the exponential of the penalty function, $\exp\{\phi(\hat{\mathbf{y}}_k, \mathbf{h}(\mathbf{x}_k); \boldsymbol{\Omega})\}$, acting as the measurement likelihood function $f(\hat{\mathbf{y}}_k|\mathbf{x}_k;\boldsymbol{\theta}_k)$. Here the quadratic penalty function is implicitly modeling $\hat{\mathbf{y}}_k$ as Gaussian with mean $\mathbf{h}(\mathbf{x}_k)$ and covariance matrix $\boldsymbol{\Omega}$. Here we choose $\boldsymbol{\Omega}$ to be the inverse of the Fisher information matrix (FIM) of the natural parameters, defined as [11]:

$$\mathbf{J}_{\mathbf{y}}(\mathbf{y}_k;\boldsymbol{\theta}_k) \equiv -E_{\mathbf{z}_k|\mathbf{y}_k;\boldsymbol{\theta}_k}\left\{\boldsymbol{\Delta}_{\mathbf{y}_k}^{\mathbf{y}_k} \ln f(\mathbf{z}_k|\mathbf{y}_k;\boldsymbol{\theta}_k)\right\}, \tag{13}$$

where $\boldsymbol{\Delta}_{\mathbf{y}_k}^{\mathbf{y}_k}$ denotes the matrix of second-order partial derivatives with respect to the components of $\mathbf{y}_k$.

Calculation of the FIM often requires knowledge of the true value of $\mathbf{y}_k$, however we can obtain a reasonably accurate approximation to the FIM by substituting in an estimate of $\mathbf{y}_k$. The transformation of the predicted state estimate $\mathbf{h}(\hat{\mathbf{x}}_k^-)$ is a less volatile estimate than the current measurement $\hat{\mathbf{y}}_k$, therefore we evaluate the FIM at $\mathbf{h}(\hat{\mathbf{x}}_k^-)$. Thus, for the information update we choose

$$\boldsymbol{\Omega}_{I,k}^{-1} = \mathbf{J}_{\mathbf{y}}(\mathbf{h}(\hat{\mathbf{x}}_k^-);\boldsymbol{\theta}_k). \tag{14}$$

C. Controller

In the controller, we assume that we have received observations up to time t_{k-1} and want to find $\boldsymbol{\theta}_k$ to optimize the performance of the state estimator that will include the next observation $\mathbf{z}_k$ as well as the previous observations $\mathbf{Z}_{k-1}$. The performance is characterized by the *predicted conditional Bayes risk*, which is the expected value

of the processor cost function with respect to the joint density of $\mathbf{x}_k$ and $\mathbf{z}_k$ conditioned on $\mathbf{Z}_{k-1}$ [5]:

$$R_C^{\uparrow}(\boldsymbol{\theta}_k|\mathbf{Z}_{k-1};\boldsymbol{\Theta}_{k-1}) \equiv E_k^{\uparrow}\{C\left(\hat{\mathbf{x}}(\mathbf{Z}_k),\mathbf{x}_k\right)\}, \tag{15}$$

where $E_k^{\uparrow}\{\cdot\}$ denotes expectation with respect to the joint density

$$\begin{aligned} f^{\uparrow}(\mathbf{x}_k,\mathbf{z}_k) &\equiv f(\mathbf{x}_k,\mathbf{z}_k|\mathbf{Z}_{k-1};\boldsymbol{\Theta}_k) \\ &= f(\mathbf{z}_k|\mathbf{h}(\mathbf{x}_k);\boldsymbol{\theta}_k)f^{-}(\mathbf{x}_k). \end{aligned} \tag{16}$$

For the tracking cost function, the predicted conditional Bayes risk is the trace of the predicted conditional mean square error (MSE) matrix, which is difficult to evaluate analytically. However, it can be lower bounded by the predicted conditional Cramér-Rao lower bound (PC-CRLB), which provides a (matrix) lower bound on the MSE matrix and is usually analytically tractable. It is the inverse of the predicted conditional Bayesian information matrix (PC-BIM), defined as [5]:

$$\mathbf{B}_k^{\uparrow}(\boldsymbol{\theta}_k|\mathbf{Z}_{k-1};\boldsymbol{\Theta}_{k-1}) = -E_k^{\uparrow}\left\{\boldsymbol{\Delta}_{\mathbf{x}_k}^{\mathbf{x}_k}\ln f^{\uparrow}(\mathbf{x}_k,\mathbf{z}_k)\right\}. \tag{17}$$

The PC-BIM may be expressed as the sum of a prior term and a data term as follows:

$$\begin{aligned} &\mathbf{B}_k^{\uparrow}(\boldsymbol{\theta}_k|\mathbf{Z}_{k-1};\boldsymbol{\Theta}_{k-1}) = \\ &\quad \mathbf{B}_k^{-}(\boldsymbol{\theta}_k|\mathbf{Z}_{k-1};\boldsymbol{\Theta}_{k-1}) + \mathbf{J}_k^{-}(\boldsymbol{\theta}_k|\mathbf{Z}_{k-1};\boldsymbol{\Theta}_{k-1}). \end{aligned} \tag{18}$$

We call the prior term in (18) the predicted information matrix (PIM). For Gaussian densities, the PIM is equal to the inverse of the predicted covariance matrix,

$$\mathbf{B}_k^{-}(\boldsymbol{\theta}_k|\mathbf{Z}_{k-1};\boldsymbol{\Theta}_{k-1}) = \boldsymbol{\Sigma}_k^{-}(\boldsymbol{\theta}_k|\mathbf{Z}_{k-1};\boldsymbol{\Theta}_{k-1})^{-1}. \tag{19}$$

The data term in (18) is the expected value of the FIM with respect to the predicted density $f^{-}(\mathbf{x}_k)$. The expected FIM (EFIM) is given by:

$$\mathbf{J}_k^{-}(\boldsymbol{\theta}_k|\mathbf{Z}_{k-1};\boldsymbol{\Theta}_{k-1}) \equiv E_k^{-}\{\mathbf{J}_{\mathbf{x}}(\mathbf{x}_k;\boldsymbol{\theta}_k)\}, \tag{20}$$

where $\mathbf{J}_{\mathbf{x}}(\mathbf{x}_k;\boldsymbol{\theta}_k)$ is the standard FIM with respect to the state parameters. It can be obtained from the FIM with respect to the natural parameters by the relationship [11]:

$$\mathbf{J}_{\mathbf{x}}(\mathbf{x}_k;\boldsymbol{\theta}_k) = \mathbf{H}(\mathbf{x}_k)^T\mathbf{J}_{\mathbf{y}}\left(\mathbf{h}(\mathbf{x}_k);\boldsymbol{\theta}_k\right)\mathbf{H}(\mathbf{x}_k). \tag{21}$$

The controller optimization problem is then given by

$$\boldsymbol{\theta}_k = \arg\min_{\boldsymbol{\theta}} L_{C,\boldsymbol{\Theta}}\left(\mathbf{B}_k^{\uparrow}(\boldsymbol{\theta}|\mathbf{Z}_{k-1};\boldsymbol{\Theta}_{k-1}), R_{\Theta}(\boldsymbol{\theta})\right). \tag{22}$$

The cognitive MAP-PF tracking recursion is summarized in Table I. For a specific application, we would need to specify the components of the state vector and natural parameter vector, the motion and measurement models, the sensor parameters being controlled, and the form of the controller loss function. Finally, we would need to specify the implementation details that include the type of tracker used to implement the Bayes-Markov recursion and the method for solving the controller optimization problem.

III. Software Defined Radar Example

We now demonstrate performance for a pulse-Doppler radar system in which the PRF is adjusted to optimize tracking performance, while keeping the target from being Doppler-aliased and away from the zero-Doppler clutter. Results are shown on experimentally collected data using an SDR system [9]-[10]. The experimental configuration for the data collection is shown in Figure 2. The human target walks back and forth over a five meter range and exhibits varying velocities and a fluctuating radar cross section (RCS) as it moves.

TABLE I
COGNITIVE MAP-PF TRACKING FRAMEWORK

Initialization

$$f^{+}(\mathbf{x}_0) = q(\mathbf{x}_0) \tag{23}$$

Controller Optimization

$$f^{-}(\mathbf{x}_k;\boldsymbol{\theta}) = \int q(\mathbf{x}_k|\mathbf{x}_{k-1};\boldsymbol{\theta})f^{+}(\mathbf{x}_{k-1})d\mathbf{x}_{k-1} \tag{24}$$

$$\boldsymbol{\mu}_k^{-}(\boldsymbol{\theta}) = E_k^{-}\{\mathbf{x}_k\} \tag{25}$$

$$\boldsymbol{\Sigma}_k^{-}(\boldsymbol{\theta}|\mathbf{Z}_{k-1};\boldsymbol{\Theta}_{k-1}) = E_k^{-}\left\{\left[\mathbf{x}_k-\boldsymbol{\mu}_k^{-}(\boldsymbol{\theta})\right]\left[\mathbf{x}_k-\boldsymbol{\mu}_k^{-}(\boldsymbol{\theta})\right]^T\right\} \tag{26}$$

$$\mathbf{B}_k^{-}(\boldsymbol{\theta}|\mathbf{Z}_{k-1};\boldsymbol{\Theta}_{k-1}) = \boldsymbol{\Sigma}_k^{-}(\boldsymbol{\theta}|\mathbf{Z}_{k-1};\boldsymbol{\Theta}_{k-1})^{-1} \tag{27}$$

$$\mathbf{J}_{\mathbf{y}}(\mathbf{y}_k;\boldsymbol{\theta}) = -E_{\mathbf{z}_k|\mathbf{y}_k;\boldsymbol{\theta}}\left\{\boldsymbol{\Delta}_{\mathbf{y}_k}^{\mathbf{y}_k}\ln f(\mathbf{z}_k|\mathbf{y}_k;\boldsymbol{\theta})\right\} \tag{28}$$

$$\mathbf{J}_{\mathbf{x}}(\mathbf{x}_k;\boldsymbol{\theta}) = \mathbf{H}(\mathbf{x}_k)^T\mathbf{J}_{\mathbf{y}}\left(\mathbf{h}(\mathbf{x}_k);\boldsymbol{\theta}\right)\mathbf{H}(\mathbf{x}_k) \tag{29}$$

$$\mathbf{J}_k^{-}(\boldsymbol{\theta}|\mathbf{Z}_{k-1};\boldsymbol{\Theta}_{k-1}) = E_k^{-}\{\mathbf{J}_{\mathbf{x}}(\mathbf{x}_k;\boldsymbol{\theta})\} \tag{30}$$

$$\begin{aligned} \mathbf{B}_k^{\uparrow}(\boldsymbol{\theta}|\mathbf{Z}_{k-1};\boldsymbol{\Theta}_{k-1}) &= \mathbf{B}_k^{-}(\boldsymbol{\theta}|\mathbf{Z}_{k-1};\boldsymbol{\Theta}_{k-1}) \\ &\quad +\mathbf{J}_k^{-}(\boldsymbol{\theta}|\mathbf{Z}_{k-1};\boldsymbol{\Theta}_{k-1}) \end{aligned} \tag{31}$$

$$\boldsymbol{\theta}_k = \arg\min_{\boldsymbol{\theta}} L\Big(\mathrm{tr}\left\{\mathbf{B}_k^{\uparrow}(\boldsymbol{\theta}|\mathbf{Z}_{k-1};\boldsymbol{\Theta}_{k-1})^{-1}\right\}, R_{\Theta}(\boldsymbol{\theta})\Big) \tag{32}$$

Motion Update

$$f^{-}(\mathbf{x}_k) = \int q(\mathbf{x}_k|\mathbf{x}_{k-1};\boldsymbol{\theta}_k)f^{+}(\mathbf{x}_{k-1})d\mathbf{x}_{k-1} \tag{33}$$

$$\hat{\mathbf{x}}_k^{-} = \boldsymbol{\mu}_k^{-} = E_k^{-}\{\mathbf{x}_k\} \tag{34}$$

$$\boldsymbol{\Sigma}_k^{-} = E_k^{-}\left\{\left[\mathbf{x}_k-\boldsymbol{\mu}_k^{-}\right]\left[\mathbf{x}_k-\boldsymbol{\mu}_k^{-}\right]^T\right\} \tag{35}$$

Measurement

Obtain the measurement $\mathbf{z}_k$ according to $\boldsymbol{\theta}_k$

$$\boldsymbol{\Omega}_{\mathrm{MAP},k} = \mathbf{H}(\hat{\mathbf{x}}_k^{-})\boldsymbol{\Sigma}_k^{-}\mathbf{H}(\hat{\mathbf{x}}_k^{-})^T \tag{36}$$

$$\hat{\mathbf{y}}_k = \arg\max_{\mathbf{y}} \ln f(\mathbf{z}_k|\mathbf{y};\boldsymbol{\theta}_k) + \phi\left(\mathbf{y},\mathbf{h}(\hat{\mathbf{x}}_k^{-});\boldsymbol{\Omega}_{\mathrm{MAP},k}\right) \tag{37}$$

Information Update

$$\boldsymbol{\Omega}_{I,k}^{-1} = \mathbf{J}_{\mathbf{y}}\left(\mathbf{h}(\hat{\mathbf{x}}_k^{-});\boldsymbol{\theta}_k\right) \tag{38}$$

$$f^{+}(\mathbf{x}_k) = \frac{\exp\left\{\phi\left(\hat{\mathbf{y}}_k,\mathbf{h}(\mathbf{x}_k);\boldsymbol{\Omega}_{I,k}\right)\right\}f^{-}(\mathbf{x}_k)}{\int\exp\left\{\phi\left(\hat{\mathbf{y}}_k,\mathbf{h}(\mathbf{x}_k);\boldsymbol{\Omega}_{I,k}\right)\right\}f^{-}(\mathbf{x}_k)d\mathbf{x}_k} \tag{39}$$

Track Estimate

$$\hat{\mathbf{x}}_k^{+} = \boldsymbol{\mu}_k^{+} = E_k^{+}\{\mathbf{x}_k\} \tag{40}$$

$$\boldsymbol{\Sigma}_k^{+} = E_k^{+}\left\{\left[\mathbf{x}_k-\boldsymbol{\mu}_k^{+}\right]\left[\mathbf{x}_k-\boldsymbol{\mu}_k^{+}\right]^T\right\} \tag{41}$$

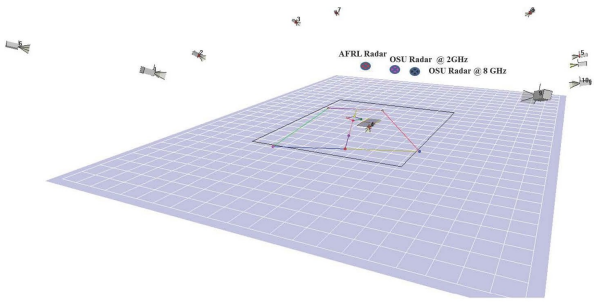

Fig. 2. **SDR Experimental Setup [10]**

The system operates at f_c = 8 GHz and transmits linear frequency modulation (LFM) pulses with bandwidth B = 500 MHz, therefore

the range resolution is 0.3m. 12,200 pulses of data were collected with a fixed PRF of 800 Hz over 15.25 s. Cognitive processing is performed "after the fact" on the stored data, with the PRF being adjusted artificially by downsampling the pulses by a factor of one to four to achieve PRFs of 800, 400, 267, and 200 Hz.

To visualize the data, we performed Hamming-windowed Doppler processing to produce a range/Doppler (RD) surface on overlapping 256-pulse coherent processing intervals (CPIs). There is strong clutter in the zero-Doppler bin and a few surrounding bins, therefore we perform "clutter-nulling" by simply discarding the data in these bins. Range and Doppler cuts at the peak RD response vs. time are shown in Figures 3 and 4. The signal-to-noise ratio (SNR) is higher when the target is closer in range and lower when it is farther away. The peak value in Doppler corresponds to the motion of the torso and there is significant micro-Doppler structure due to the motion of the arms and legs of the human subject. The peak Doppler is largest when the target is at mid-range and passes through zero when the target is at the end ranges and turning around. The peak Doppler has a maximum value of about 135 Hz, thus we have room to lower the PRF without causing Doppler aliasing.

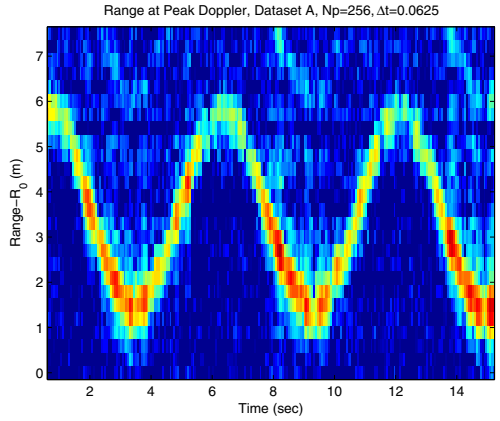

Fig. 3. **Range vs. time**

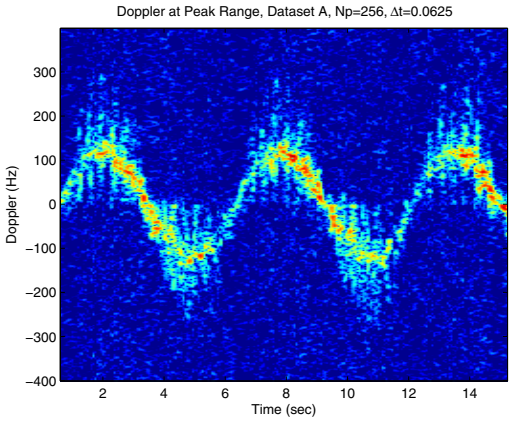

Fig. 4. **Doppler vs. time**

For the cognitive processing, each scan consists of an N_p = 128 pulse CPI at the designated PRF, thus the scan interval varies with the PRF,

$$\Delta t_k = \frac{N_p}{PRF_k}. \tag{42}$$

A. Model

The target kinematic parameters that we wish to estimate and track are the range r_k and velocity v_k. Let $\boldsymbol{\rho}_k = \begin{bmatrix} r_k & v_k \end{bmatrix}^T$ denote the kinematic parameter vector. The SDR observes the target via the natural radar parameters of range r_k and Doppler frequency f_k. Let $\boldsymbol{\eta}_k = \begin{bmatrix} r_k & f_k \end{bmatrix}^T$ denote the natural radar parameter vector. The natural parameters are related to the kinematic parameters by the linear transformation

$$\boldsymbol{\eta}_k = \mathbf{T}\boldsymbol{\rho}_k, \tag{43}$$

where

$$\mathbf{T} = \begin{bmatrix} 1 & 0 \\ 0 & -\dfrac{2f_c}{c} \end{bmatrix}. \tag{44}$$

To calculate the FIM, we need to know the post-processing SNR, therefore we track the SNR (in dB) along with the kinematic parameters. Let s_k denote the post-processing SNR in dB:

$$s_k = 10\log_{10}(SNR_k). \tag{45}$$

We augment the kinematic and natural parameters with s_k to obtain:

$$\mathbf{x}_k = \begin{bmatrix} r_k & v_k & s_k \end{bmatrix}^T \tag{46}$$

$$\mathbf{y}_k = \begin{bmatrix} r_k & f_k & s_k \end{bmatrix}^T. \tag{47}$$

The natural parameter vector is related to the target state vector by the mapping

$$\mathbf{y}_k = \mathbf{h}(\mathbf{x}_k) = \mathbf{H}\mathbf{x}_k, \tag{48}$$

where

$$\mathbf{H} = \begin{bmatrix} 1 & 0 & 0 \\ 0 & -\dfrac{2f_c}{c} & 0 \\ 0 & 0 & 1 \end{bmatrix}. \tag{49}$$

The sensor parameter θ is the PRF. The sensor cost function restricts the allowable PRFs to a finite set. The cost is zero when the PRF is one of the pre-defined values and infinite otherwise:

$$R_\Theta(\theta) = \begin{cases} 0 & \theta \in \{800, 400, 267, 200\} \\ \infty & \text{otherwise.} \end{cases} \tag{50}$$

We assume an initial state distribution of the form $\mathbf{x}_0 \sim N(\bar{\mathbf{x}}_0, \boldsymbol{\Omega}_0)$ and a nearly constant velocity motion model with additive white Gaussian noise of the form:

$$\mathbf{x}_k = \mathbf{F}(\Delta t_k)\mathbf{x}_{k-1} + \mathbf{v}_k, \tag{51}$$

where

$$\mathbf{F}(\Delta t_k) = \begin{bmatrix} 1 & \Delta t_k & 0 \\ 0 & 1 & 0 \\ 0 & 0 & 1 \end{bmatrix} \tag{52}$$

and $\mathbf{v}_k \sim N(\mathbf{0}, \mathbf{Q}(\Delta t_k))$ with $\mathbf{Q}(\Delta t_k)$ determined through empirical data analysis to have the form [12]:

$$\mathbf{Q}(\Delta t_k) = \begin{bmatrix} \sigma_r^2 \Delta t_k^2 & 0 & 0 \\ 0 & \sigma_v^2 \sqrt{\Delta t_k} & 0 \\ 0 & 0 & \sigma_s^2 \Delta t_k \end{bmatrix}, \tag{53}$$

where σ_r^2, σ_v^2, and σ_s^2 are constants determined empirically.

Let $RD_k(\boldsymbol{\eta}; \theta_k)$ denote the RD surface obtained from processing $\mathbf{z}_k$, which was collected with PRF = θ_k. Empirical data analysis gives us the following approximations to the likelihood function and FIM:

$$\ln f(\mathbf{z}_k|\mathbf{y}; \theta_k) \approx 10\log_{10} RD_k(\boldsymbol{\eta}; \theta_k) \tag{54}$$

$$\mathbf{J}_\mathbf{y}(s_k; \theta_k) \approx \begin{bmatrix} C_r 10^{s_k/10} & 0 & 0 \\ 0 & C_f \dfrac{10^{s_k/10}}{\theta_k^2} & 0 \\ 0 & 0 & C_s \end{bmatrix}, \tag{55}$$

where C_r, C_f, and C_s are constants determined empirically.

Track estimation performance is characterized by the root MSE (RMSE). Let ξ_r and ξ_v denote the RMSE in range and velocity, respectively. PRF affects the SDR system performance in several conflicting ways:

- As PRF decreases, Δt_k increases and motion model uncertainty in $\mathbf{Q}(\Delta t_k)$ increases. This makes both range and velocity tracking resolution poorer (ξ_r and ξ_v larger).
- As PRF decreases, the Doppler bin width (PRF/128) in the RD surface decreases. This improves the Doppler measurement resolution (as reflected in the frequency entry of the FIM) and makes velocity tracking resolution better (ξ_v smaller).
- The zero-Doppler clutter occupies a few Doppler bins regardless of PRF. As PRF decreases and Doppler bin width decreases, the target Doppler bin, which has index I_D, moves away from the zero-Doppler clutter.
- As PRF decreases, there will be Doppler aliasing if the absolute value of target Doppler is larger than PRF/2.

The controller optimization problem finds maximum PRF (minimum scan time) that keeps the target out of the zero-Doppler clutter and achieves a velocity resolution goal, without Doppler aliasing. Prevention of Doppler aliasing takes priority and we specify the clutter and resolution goals of the form $I_D \geq I_{D,min}$ and $\xi_v \leq \xi_{v,max}$.

B. Implementation

We use a Kalman filter for the tracking method. The MAP-PF guided detector obtains range and Doppler estimates from the peak of the RD surface. We estimate the noise from the median of the RD surface at the estimated range, and compute the SNR (in dB) as the value at the peak of the RD surface minus the noise (in dB).

In the controller optimization step, we start with the largest PRF and, as long as we are not Doppler aliased, keep decreasing until the resolution goal and target distance from clutter goals are met. For each PRF, we compute a motion update and calculate the PC-CRLB. For the linear Gaussian model assumed here, the PC-CRLB is calculated in the same manner as the posterior covariance matrix in the Kalman filter. From the motion update, we form a 1.5 confidence interval on the Doppler. If any portion of the confidence interval is aliased, then we stop and keep the previous PRF. It there is no aliasing, then we check the resolution goal by comparing the standard deviation of the velocity component of the PC-CRLB to our goal value. We also check to see how far away the predicted Doppler estimate is from the zero-Doppler clutter. If both goals are achieved, then we stop, otherwise we decrease the PRF and continue. The implementation details are given in Table II.

C. Results

Figure 5 shows a screen shot of the display that is produced as the tracker runs. The display consists of nine panels. Upper left: RD surface at the current scan. Middle left: clutter-nulled RD surface with penalty function at the current scan. The yellow ellipse is the 2σ ellipse of the likelihood penalty function centered on the predicted range and Doppler. The magenta ellipse is the 2σ ellipse of the measurement CRLB centered on the measurement obtained from the peak of the penalized RD surface. Lower left: 2σ ellipses of the predicted and posterior densities for the range and velocity. Middle three panels: range, velocity, and SNR tracks with 2σ confidence intervals, and the measurement provided to the tracker. Upper right: predicted maximum and mean target Doppler bins with goals. Middle right: velocity RMSE vs. time with performance goal. Lower right: PRF vs. time.

TABLE II
COGNITIVE SDR TRACKING IMPLEMENTATION

Initialization

$\hat{\mathbf{x}}_0 = \boldsymbol{\mu}_0$

$\hat{\mathbf{P}}_0 = \boldsymbol{\Sigma}_0$

Controller Optimization (θ = PRF)

Start with the largest θ. For each θ compute:

$\mathbf{x}_k^-(\theta) = \mathbf{F}(\theta)\hat{\mathbf{x}}_{k-1}$

$\mathbf{P}_k^-(\boldsymbol{\theta}) = \mathbf{F}(\theta)\hat{\mathbf{P}}_{k-1}\mathbf{F}(\theta)^T + \mathbf{Q}(\theta)$

$\mathbf{R}_k(\theta) = \mathbf{J}_{\mathbf{y}}\left(s_k^-(\theta);\theta\right)$

$\mathbf{G}_k(\theta) = \mathbf{P}_k^-(\theta)\mathbf{H}^T\left[\mathbf{H}\mathbf{P}_k^-(\theta)\mathbf{H}^T + \mathbf{R}_k(\theta)\right]^{-1}$

$\mathbf{B}_k^{\uparrow}(\theta)^{-1} = \mathbf{P}_k^-(\boldsymbol{\theta}) - \mathbf{G}_k(\boldsymbol{\theta})\mathbf{H}\mathbf{P}_k^-(\boldsymbol{\theta})$

$\hat{f}_D(\theta) = v_k^-(\theta)\left(-\dfrac{2f_c}{c}\right)$

$\sigma_D(\theta) = \sqrt{\left[\mathbf{P}_k^-(\boldsymbol{\theta})\right]_{22}}\left(\dfrac{2f_c}{c}\right)$

$f_D(\theta) \in \left\{\hat{f}_D(\theta) \pm 1.5\sigma_D(\theta)\right\}$

$\xi_v(\theta) = \sqrt{\left[\mathbf{B}_k^{\uparrow}(\theta)^{-1}\right]_{22}}$

If $\max(|f_D(\theta)|) > \theta/2$ then *Doppler aliased*; stop and use previous θ

If bin index of $|\hat{f}_D(\theta)| > I_{D,min}$ then *away from clutter*

If $\xi_v(\theta) < \xi_{v,min}$, then *resolution achieved*

If *away from clutter* and *resolution achieved* then stop, otherwise go to next θ

$\theta_k = \theta$

Motion Update

$\hat{\mathbf{x}}_k^- = \mathbf{F}(\theta_k)\hat{\mathbf{x}}_{k-1}$

$\hat{\mathbf{P}}_k^- = \mathbf{F}(\theta_k)\hat{\mathbf{P}}_{k-1}\mathbf{F}(\theta_k)^T + \mathbf{Q}(\theta_k)$

Measurement

Obtain the SDR data $\mathbf{z}_k$ with PRF = θ_k and RD process to get $RD_k(\boldsymbol{\eta};\theta_k)$

$\hat{\boldsymbol{\eta}}_k = \arg\max_{\boldsymbol{\eta}} 10\log_{10} RD_k(\boldsymbol{\eta};\theta_k) + \phi(\boldsymbol{\eta}, \mathbf{T}\hat{\boldsymbol{\rho}}_k^-; \mathbf{T}\boldsymbol{\Sigma}_{\boldsymbol{\rho}_k}^-\mathbf{T}^T)$

$\hat{n}_k =$ median of $10\log_{10} RD_k(\boldsymbol{\eta};\theta_k)$ across Doppler at $\hat{r}_k$

$\hat{s}_k^- = 10\log_{10} RD(\hat{\boldsymbol{\eta}}_k;\theta_k) - \hat{n}_k$

Information Update and Track Estimate

$\mathbf{R}_k = \mathbf{J}_{\mathbf{y}}\left(\hat{s}_k^-;\theta_k\right)$

$\mathbf{G}_k = \hat{\mathbf{P}}_k^-\mathbf{H}^T\left[\mathbf{H}\hat{\mathbf{P}}_k^-\mathbf{H}^T + \mathbf{R}_k\right]^{-1}$

$\hat{\mathbf{x}}_k = \hat{\mathbf{x}}_k^- + \mathbf{G}_k\left(\hat{\mathbf{y}}_k - \mathbf{H}\hat{\mathbf{x}}_k^-\right)$

$\hat{\mathbf{P}}_k = \hat{\mathbf{P}}_k^- - \mathbf{G}_k\mathbf{H}\hat{\mathbf{P}}_k^-$

In the operation of the MAP-PF tracker, guided detection in the form of a penalized RD surface guides the detector to the right place and eliminates distracting clutter peaks that might cause false detections. The strictness of the penalty function varies according to conditions reported by the tracker. This is a critical step that allows the tracker to maintain track during low SNR conditions and when the target is moving quickly and contributes to the overall performance of the cognitive SDR tracking system. The optimal PRF varies between

267 and 800 Hz. There is no Doppler aliasing and the target is kept away from the clutter. The velocity resolution performance goal is achieved except for a few low SNR scans.

IV. Summary

In this paper, we have developed a cognitive radar tracking system based on the MAP-PF methodology that allows us to cognitively control both the sensor and processor. The framework mimics the cognitive *perception-action cycle* and includes *sensing* in the sensor; *processing* in the detector and tracker; *perception* in the conversion of sensor data to the posterior density of the state vector; *memory* of all the past data in the posterior density; *attention* in the penalty function of the guided detector, which focuses the detector on the relevant region of the detection surface; *prediction* in the PC-BIM, which predicts the performance of the next measurement; and *decision-making* in the controller, which decides on the next values for the sensor parameters based on the predicted performance.

We demonstrated performance for a pulse-Doppler radar system in which the pulse repetition frequency was adjusted to optimize tracking performance, while keeping the target from being Doppler-aliased and away from the zero-Doppler clutter. Results were shown on experimentally collected data using an SDR system. Plans are underway to repeat the experiment in real time.

References

[1] S. Haykin, Y. Xue, and M. P. Setoodeh, "Cognitive radar: step toward bridging the gap between neuroscience and engineering," *Proc. IEEE*, vol. 100, no. 11, pp. 3102-3130, November 2012.

[2] S. Haykin, *Cognitive Dynamic Systems (Perception-Action Cycle, Radar, and Radio)*. Cambridge University Press, 2012.

[3] J. R. Guerci, *Cognitive Radar: The Knowledge Aided Fully Adaptive Approach*. Reading, MA: Artech House, 2010.

[4] F. Gini and M. Rangaswamy, Eds., *Knowledge Based Radar Detection, Tracking, and Classification*. Hoboken, NJ: Wiley, 2008.

[5] K. L. Bell, C. J. Baker, G. E. Smith, J. T. Johnson, and M. Rangaswamy, "Fully Adaptive Radar for Target Tracking Part I: Single Target Tracking," *2014 IEEE Radar Conf.*, Cincinnati, OH, pp. 303-308, May 2014.

[6] K. L. Bell, C. J. Baker, G. E. Smith, J. T. Johnson, and M. Rangaswamy, "Fully Adaptive Radar for Target Tracking Part II: Target Detection and Track Initiation," *2014 IEEE Radar Conf.*, Cincinnati, OH, pp. 309-314, May 2014.

[7] R. E. Zarnich, K. L. Bell, and H. L. Van Trees, "A Unified Method for Measurement and Tracking of Multiple Contacts from Sensor Array Data," *IEEE Trans. Sig. Proc.*, vol. 49, no.12, pp. 2950-2961, Dec. 2001.

[8] L. D. Stone, R. L. Streit, T. L. Corwin, and K. L. Bell, *Bayesian Multiple Target Tracking, 2nd Ed.* Norwood, MA: Artech House, 2014.

[9] K. B. Stewart, M. T. Frankford, N. Majurec, and J. T. Johnson, "Software Defined Radar for Cognitive Applications," *URSI National Radio Science Meeting*, 2012.

[10] J. Park, "Multi-Frequency Radar Signatures of Human Motion: Measurements and Models," Ph.D. Dissertation, The Ohio State University, 2012.

[11] H. L. Van Trees and K. L. Bell with Z. Tian, *Detection, Estimation, and Modulation Theory, Part I, 2nd Ed.* Hoboken, NJ: Wiley, 2013.

[12] K. L. Bell, C. J. Baker, G. E. Smith, and J. T. Johnson, "Fully Adaptive Radar." AFRL Tech. Report AFRL-RY-WP-TR-2014-0072, March 2014.

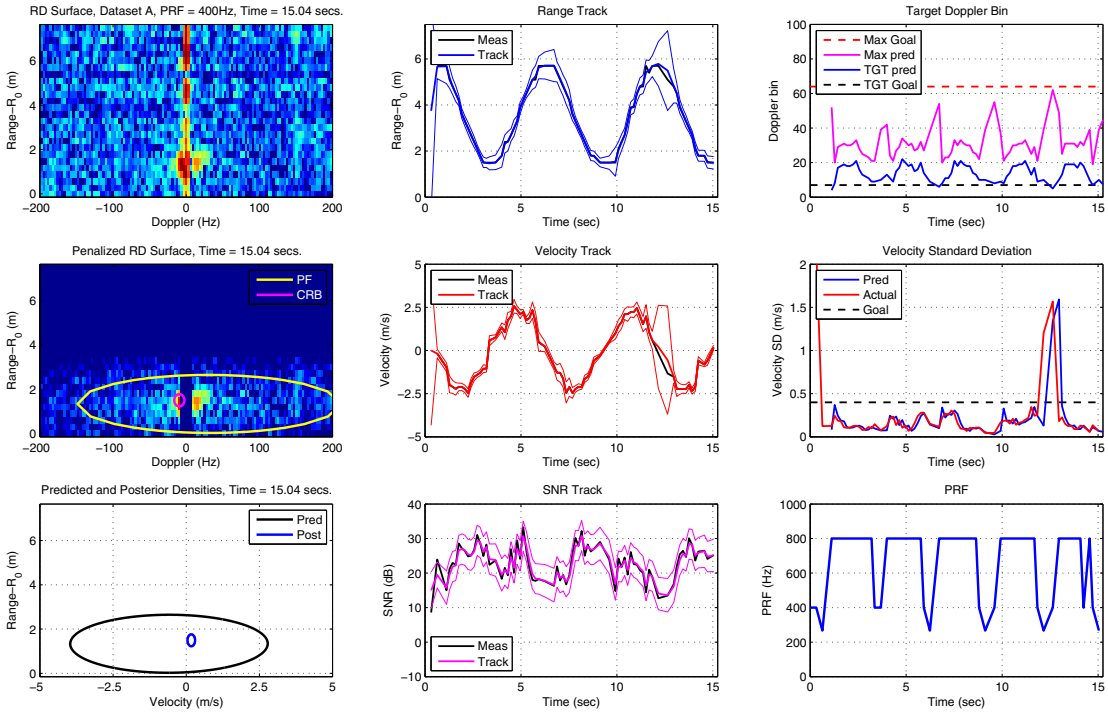

Fig. 5. **Cognitive SDR Tracking Display**